

“Trojan horse” method applied to ${}^2\text{H}({}^6\text{Li},\alpha){}^4\text{He}$ at astrophysical energies

C. Spitaleri,^{1,2,*} S. Typel,³ R. G. Pizzone,^{1,2} M. Aliotta,⁴ S. Blagus,⁵ M. Bogovac,⁵ S. Cherubini,⁶ P. Figuera,¹ M. Lattuada,^{1,7} M. Milin,⁵ D. Miljanić,⁵ A. Musumarra,^{1,2} M. G. Pellegriti,^{1,2} D. Rendić,⁵ C. Rolfs,⁷ S. Romano,^{1,2} N. Soić,⁵ A. Tumino,^{1,8} H. H. Wolter,³ and M. Zadro⁵

¹Laboratori Nazionali del Sud-INFN, Catania, Italy

²Dipartimento di Metodologie Fisiche e Chimiche per l'Ingegneria, Università di Catania, Catania, Italy

³Ludwig-Maximilians Universität München, München, Germany

⁴Ruhr-Universität Bochum, Bochum, Germany

⁵Institut-Rudjer Bošković, Zagreb, Croatia

⁶Université Catholique de Louvain, Louvain-la-Neuve, Belgium

⁷Dipartimento di Fisica e Astronomia, Università di Catania, Catania, Italy

⁸Centro Siciliano di Fisica Nucleare e Struttura della Materia, Catania, Italy

(Received 19 October 2000; published 17 April 2001)

The ${}^6\text{Li}({}^6\text{Li},\alpha){}^4\text{He}$ three-body reaction has been studied in a kinematically complete experiment at $E_{6,\text{Li}} = 6$ MeV, from which indirect information on the ${}^2\text{H}({}^6\text{Li},\alpha){}^4\text{He}$ two-body reaction at $13 \leq E_{\text{c.m.}} \leq 750$ keV has been extracted by applying the *Trojan horse* method. The method used a recent improved formulation. The derived astrophysical $S(E)$ factor for the two-body process is compared with that obtained from direct experiments.

DOI: 10.1103/PhysRevC.63.055801

PACS number(s): 26.20.+f, 21.10.Pc, 24.50.+g, 25.70.Hi

I. INTRODUCTION

In recent years various indirect methods (e.g., Coulomb dissociation [1,2] and transfer reactions [1,3–6]) have been employed in determination of reaction cross sections for nuclear astrophysics. Among these methods, the so-called Trojan horse method (THM) [7] seems to be particularly suited for extracting information about charged-particle-induced cross sections at the low energies encountered in astrophysics, because the method overcomes the effects due to the entrance channel Coulomb barrier. This method has already been used to determine the cross sections for the ${}^6\text{Li}(d,\alpha){}^4\text{He}$ [8] and the ${}^7\text{Li}(p,\alpha){}^4\text{He}$ [9,10] reactions. The extracted astrophysical $S(E)$ factors have been compared with those from direct measurements [11,12]. The ${}^7\text{Li}(p,\alpha){}^4\text{He}$ $S(E)$ -factor seems to be in good agreement with direct data over the energy region investigated. In the case of the ${}^6\text{Li}(d,\alpha){}^4\text{He}$ reaction, good agreement was obtained in the energy range $E_{\text{c.m.}} = 0.15\text{--}1.0$ MeV, but not at lower energies. Also the possibility of an application of the THM to the ${}^{12}\text{C}(\alpha,\alpha){}^{12}\text{C}$ reaction [13] has been recently investigated.

In this paper we present an improved experimental study of the ${}^6\text{Li}({}^6\text{Li},\alpha){}^4\text{He}$ reaction performed with the aim of extracting the $S(E)$ factor for the reaction ${}^6\text{Li}(d,\alpha){}^4\text{He}$ at energies lower than 150 keV. To accomplish this aim a more detailed treatment of the THM [14], based on distorted wave and plane wave Born approximation formulations of direct reaction theory, is used here in a simple approach. In particular, the better quality of the present data allows us to investigate the reaction at the ultralow energies.

II. THEORY

The basic assumptions of the THM have already been discussed extensively elsewhere [7,9] and a detailed theoretical derivation of the formalism employed can be found in [14]. The method is based on the quasifree (QF) reaction mechanism [15], which allows us to derive indirectly the cross section of a two-body reaction

$$A + x \rightarrow C + c \quad (1)$$

from the measurement of a suitable three-body process

$$A + a \rightarrow C + c + b. \quad (2)$$

The nucleus a is considered to be dominantly composed of clusters x and b . After the breakup of a due to the interaction with A the two-body reaction occurs between the transferred particle x and nucleus A whereas nucleus b does not participate and acts as a spectator. The energy in the entrance channel $A + a$ can be chosen above the height of the Coulomb barrier, so as to avoid a reduction in cross section. At the same time the effective energy of the reaction between A and x can be relatively small because the Fermi motion of x inside a can compensate at least partially for the $A + a$ relative motion. Since the transferred particle x is hidden inside the nucleus a and the collision of A and x takes place in the nuclear interaction region, the two-body reaction is almost free of Coulomb suppression and, at the same time, not affected by electron screening effects.

For the given breakup reaction the relevant T -matrix element T_{fi} entering the cross section is conveniently calculated in the postform distorted wave Born approximation (DWBA)

$$T_{fi} = \langle \chi_{Bb}^{(-)} \Psi_{Cc}^{(-)} \phi_b | V_{xb} | \chi_{Aa}^{(+)} \phi_a \phi_a \rangle. \quad (3)$$

*Permanent address: Laboratori Nazionali del Sud-INFN-via S. Sofia, 44-95123 Catania, Italy

The internal wave functions of nuclei A , a and b are denoted by ϕ_A , ϕ_a , and ϕ_b , respectively. The distorted waves $\chi_{Aa}^{(+)}$ and $\chi_{Bb}^{(-)}$ describe the relative motion in the initial and final channel, where B stands for the $C+c$ system. $\Psi_{Cc}^{(-)}$ is the full scattering wave function for the two-body reaction $C+c \rightarrow A+x$ that is the inverse of the reaction of astrophysical interest.

A crucial step is the surface approximation that has been discussed in Ref. [14] by considering the structure of the T -matrix element. It means to use the asymptotic form of the wave function $\Psi_{Cc}^{(-)}$ in the final channel outside a radius R . Then a direct relation of T_{fi} to the S -matrix elements of the two-body reaction can be established. To obtain simple expressions a further plane wave (PW) approximation for the relative motion of the initial $A+a$ and the final $B+b$ channels is used. This seems to be a crude approximation at first sight, but it mainly affects the absolute magnitude of the cross section. However, we are interested in extracting the energy dependence of the astrophysically relevant two-body cross section. A change of the projectile energy could affect the cross section strongly, but this energy is fixed in the experiment. Since the momenta of the particles in the final state are quite large for a large Q value and cover only a small range of the total available three-body phase space, the energy dependence is not expected to be strongly affected by the replacement of distorted waves by plane waves. At the same time, the interaction in the final state between the detected particles C and c , where the aim is to reach very small energies, is fully taken into account.

Applying the above approximations one obtains the three-body cross section as

$$\frac{d^3\sigma}{dE_C d\Omega_C d\Omega_c} = K_F |W(\vec{Q}_{Bb})|^2 \frac{16\pi^2}{(k_{Ax} Q_{Aa})^2} \frac{v_{Cc}}{v_{Ax}} \frac{d\sigma^{\text{TH}}}{d\Omega_{Ax}} \quad (4)$$

with the kinematic factor

$$K_F = \frac{\mu_{Aa} m_C}{(2\pi)^5 \hbar^7} \frac{p_C p_c^3}{p_{Aa}} \left[\left(\frac{\vec{p}_{Bb}}{\mu_{Bb}} - \frac{\vec{p}_{Cc}}{m_c} \right) \cdot \frac{\vec{p}_c}{p_c} \right]^{-1} \quad (5)$$

with the total (nuclear+Coulomb) S -matrix elements S_1 for the reaction $C+c \rightarrow A+x$ where $\delta_{(Ax)(Cc)}$ is the Kronecker symbol. It has the form of a usual two-body cross section except for the functions

$$J_l^{(\pm)} = k_{Ax} Q_{Aa} \int_R^\infty dr r j_l(Q_{Aa} r) u_l^{(\pm)}(k_{Ax} r), \quad (12)$$

which are a consequence of the off-shell nature of the two-body process. In this expression spherical Bessel functions j_l and Coulomb wave functions $u^{(\pm)} = e^{\mp i\sigma_l}(G_l \pm iF_l)$ appear.

in standard notation for (reduced) masses, momenta, and velocities. The quantities \vec{Q}_{Aa} and \vec{Q}_{Bb} in Eq. (4) are given by

$$\vec{Q}_{Aa} = \vec{k}_{Aa} - \frac{m_A}{m_A + m_z} \vec{k}_{Bb}, \quad (6)$$

$$\vec{Q}_{Bb} = \vec{k}_{Bb} - \frac{m_b}{m_b + m_z} \vec{k}_{Aa}, \quad (7)$$

with the relative momenta $\hbar \vec{k}_{Aa}$ and $\hbar \vec{k}_{Bb}$ in the entrance and exit channels, respectively. The momentum amplitude W is introduced by a Fourier transformation

$$V_{xb}(r_{xb}) \phi_a(\vec{r}_{xb}) = \int \frac{d^3q}{(2\pi)^3} W(\vec{Q}_{Bb}) \exp(i\vec{q} \cdot \vec{r}_{xb}) \phi_c \phi_b \quad (8)$$

of the product of the ground state wave function ϕ_a and the interaction potential V_{xb} . It is directly related to the momentum distribution Φ_z of the transferred nucleus x in the ‘‘Trojan horse’’ a by

$$W(\vec{Q}_{Bb}) = \left(E_a - \frac{\hbar^2 Q_{Bb}^2}{2\mu_{xb}} \right) \Phi_a(\vec{Q}_{Bb}) \quad (9)$$

with the binding energy $E_a < 0$. The momentum $\hbar \vec{Q}_{Bb}$ is directly related to the momenta of the spectator and transferred particle after the breakup. Neglecting the binding energy of the nuclei, the argument of W can be well approximated by

$$\vec{Q}_{Bb} \approx \vec{k}_{xb}. \quad (10)$$

For a target a at rest this is just the negative of the spectator recoil k_b or the momentum k_x of the transferred particle x . Of course, in the actual calculation the full expression for \vec{Q}_{Bb} is used.

The ‘‘Trojan-horse’’ cross section is

$$\frac{d\sigma^{\text{TH}}}{d\Omega_{Ax}}(C \rightarrow Ax) = \frac{1}{4k_{Cc}^2} \left| \sum_l (2l+1) P_l(\hat{Q}_{Aa} \cdot \hat{k}_{Cc}) [S_l J_l^{(+)} - \delta_{(Ax)(Cc)} J_l^{(-)}] \right|^2 \quad (11)$$

The cutoff radius R (due to the surface approximation) is usually chosen as the sum of the radii of nuclei A and x . The argument of the Legendre polynomial P_l in Eq. (4) is just the cosine of the c.m. scattering angle of the two-body reaction.

The expression (4) for the three-body breakup cross section resembles the result of a plane wave impulse approximation (PWIA) [16] where the cross section is factorized as a product of a kinematic factor K_F , the momentum distribution Φ_a of the spectator inside nucleus a , and the usual two-body cross section taken on-shell. In the PWBA off-shell effects enter both in the momentum distribution and in the

two-body cross section. Since the Coulomb interaction for the two-body process is taken fully into account, we can extract the low-energy behavior of the three-body cross section due to the reduction of the Coulomb barrier by investigating the behavior of the integrals $J_l^{(\pm)}$.

For large radii the integrand in Eq. (12) is a product of two oscillating functions of unit amplitude and thus the integral does not converge in general. Only by deviating the path of integration into the complex r plane can a finite result be obtained. However, an exact numerical computation becomes rather involved. Here we will use a simple approximation. For small energies E_{Ax} in the $A+x$ channel, i.e., small k_{Ax} and a large Sommerfeld parameter η_{Ax} , the irregular Coulomb function G_l in $u_l^{(\pm)}$ increases rapidly for small radii and the main contribution arises from radii close to the cutoff radius R . Thus we use

$$J_l^{(\pm)} \propto k_{Ax} Q_{Aa} R^2 j_l(Q_{Aa} R) u_l^{(\pm)}(k_{Ax} R) \quad (13)$$

as a first approximation that contains the essential dependence on the energy E_{Ax} . Since the quantity Q_{Aa} is almost constant for small Q_{Bb} (i.e., in the peak of the momentum distribution) the dependence of the functions $J^{(\pm)}$ on the energy E_{Ax} is given by $k_{Ax} u_l^{(\pm)}(k_{Ax} R)$. The analysis is simplified if the reaction of astrophysical interest is a nonelastic two-body process with different initial and final channels such that the $J_l^{(-)}$ term in Eq. (11) is not present. Assuming that only one partial wave l contributes dominantly to the cross section, we find in this case

$$\frac{d^3\sigma}{dE_c d\Omega_c d\Omega_c} = K_F |W(\hat{Q}_{Bb})|^2 \frac{v_{Cc}}{v_{Ax}} P_l^{-1} C_l \frac{d\sigma_l}{d\Omega_{Ax}} (Cc \rightarrow Ax), \quad (14)$$

with the usual on-shell two-body cross section $d\sigma_l/d\Omega_{Ax}$ for the reaction $C+c \rightarrow A+x$ in partial wave l and a constant C_l . The essential feature is the appearance of the Coulomb penetrability factor

$$P_l(k_{Ax} R) = \frac{1}{G_l^2(k_{Ax} R) + F_l^2(k_{Ax} R)}, \quad (15)$$

which compensates for the strong suppression in the two-body cross section at small energies due to Coulomb repulsion. The expression (14) corresponds to the heuristic approach in PWIA where one also corrects the extracted two-body cross section for the effect of Coulomb penetration. Because of the factor C_l and the surface approximation, the two-body cross section can only be obtained with an arbitrary normalization but the essential energy dependence can be extracted. Absolute cross sections can be obtained by a comparison to direct data available for most reactions of astrophysical interest for energies at least above the Coulomb barrier.

In the case of ${}^6\text{Li}({}^6\text{Li}, \alpha\alpha){}^4\text{He}$ process considered here, the ${}^6\text{Li}$ target can be assumed to break up dominantly into its constituent clusters α and d whereby the α particle is regarded as a spectator to the ${}^2\text{H}({}^6\text{Li}, \alpha){}^4\text{He}$ virtual reaction. Appropriate kinematic conditions can be selected so that the

Fermi motion of the deuteron inside ${}^6\text{Li}$ compensates, at least partially, for the beam velocity. The ${}^2\text{H}({}^6\text{Li}, \alpha){}^4\text{He}$ reaction can then take place at low interaction energies, in principle down to zero energy. Of course, due to the symmetry of the entrance channel, a similar QF process occurs, where the target and the projectile exchange their roles. In the case of projectile breakup the spectator will move on with almost the same velocity as before the occurrence of the reaction. The two cases for the QF breakup can be well distinguished experimentally due to the different kinematical properties of the α particles in the final state, which is reflected, e.g., in their emission angles. In the following we will discuss mainly the target breakup but similar considerations apply to the projectile breakup. Since we have identical particles in the initial as well as in the final state, symmetrization effects in both channels have usually to be included in the calculation. However, in the theoretical treatment of the reaction we have neglected these effects. On the one hand this error will hardly be larger than the errors from other approximations employed, on the other hand the reaction takes places without a large overlap of the particles, cf. the surface approximation for the T -matrix element and the low energies in the reaction relevant to astrophysics, reducing the importance of possible corrections.

In general, one can imagine various reaction mechanisms that can lead to three α particles in the final state, e.g., the formation of compound states or other nondirect processes. However, their contribution to the measured cross section will be only a background effect with a careful selection of the covered phase space in our experiment, because they show a different dependence on energies and scattering angles as compared to the QF process. Experimental evidence for a QF contribution in the ${}^6\text{Li}({}^6\text{Li}, \alpha\alpha){}^4\text{He}$ process has been obtained in a wide energy range [17–22]. From these measurements it was observed that the QF mechanism is dominant even at low energies mainly because of the high Q value ($=20.896$ MeV) that results in a high momentum transfer. Sequential decay processes, which are usually favored in three-body reactions, have been shown to be less important in a large part of the selected phase-space region at those energies [22].

The α - d momentum distribution in ${}^6\text{Li}$ has been widely studied both in the PWIA and the DWIA [18,22]. The most relevant result of these studies is that the two approaches have been found to give similar shapes for the α - d momentum distribution. Once the ${}^6\text{Li}$ ground-state momentum distribution is known, Eq. (14) can be inverted to obtain the two-body cross section assuming a dominance of a particular partial wave. In the more general case one has to use the full expression (4). One expects a maximum in the cross section at the kinematic conditions where the spectator energy E_α is close to zero (assuming the Trojan horse ${}^6\text{Li}$ at rest), which reflects the α particle momentum distribution in ${}^6\text{Li}$ showing a maximum at $p_\alpha = 0$, due to the s -wave α - d relative motion. For the momentum distribution of the ${}^6\text{Li}$ ground state we use the function

$$|\Phi_{\text{Li}}(q)|^2 = \frac{e^{-x}}{1+x} \quad \text{with} \quad x = \frac{q^2}{3555 \text{ fm}^{-2}}, \quad (16)$$

which has also been used in the analysis of the elastic α - ^{12}C scattering in the THM with the $^6\text{Li}(^{12}\text{C},2\alpha)\alpha$ reaction [9]. It has been obtained in a simple α - d potential model of the ^6Li ground state with a binding energy of $E_{\text{Li}} = -1.475$ MeV. The shape of the momentum distribution has a full width at half maximum of 73 MeV/ c . This is consistent with the determination from various experiments [18]. Detection angles for the outgoing α particles can be calculated from three-body kinematics under the condition $E_{\alpha}(\text{spectator})=0$. They are referred to as the *quasifree angles*. Finally, we recall that the d - ^6Li relative energy (i.e., the center-of-mass energy for the two-body subsystem) is defined in the so-called postcollision prescription as

$$E_{\text{c.m.}} = E_{\alpha_1\alpha_2} - Q, \quad (17)$$

where Q ($=22.372$ MeV) is the Q value for the two-body $^2\text{H}(^6\text{Li},\alpha)^4\text{He}$ reaction. The α particle emission angle θ_{cm} in the d - ^6Li center-of-mass system can be calculated according to the relationship [23]

$$\theta_{\text{c.m.}} = \arccos \frac{(\vec{v}_{\text{Li}} - \vec{v}_d) \cdot (\vec{v}_{\alpha_1} - \vec{v}_{\alpha_2})}{|\vec{v}_{\text{Li}} - \vec{v}_d| |\vec{v}_{\alpha_1} - \vec{v}_{\alpha_2}|}, \quad (18)$$

where the vectors \vec{v}_{Li} , \vec{v}_d , \vec{v}_{α_1} , and \vec{v}_{α_2} are the velocities of the projectile, the transferred deuteron, and the two detected α particles, respectively.

III. EXPERIMENTAL SETUP

The experiment was performed using the EN Tandem Van de Graaff accelerator of the Institut Ruder Bošković in Zagreb. A $^6\text{Li}^{2+}$ beam at 6 MeV was used to bombard an isotopically enriched $^6\text{Li}_2\text{O}$ target ($125 \mu\text{g}/\text{cm}^2$), evaporated onto $20 \mu\text{g}/\text{cm}^2$ carbon backing and oriented with its surface normal at 50° with respect to the beam axis. The beam current ranged between 10 and 15 particle nA. The beam spot on target after collimation had a diameter of about 2 mm. A silicon detector, placed at $\theta=40^\circ$, was used to detect the elastically scattered particles, thus allowing for a continuous monitoring of the target thickness during the experiment.

Since the Q value for $^6\text{Li}(^6\text{Li},\alpha\alpha)^4\text{He}$ is much larger than that for other possible three-body reactions occurring on lithium, carbon, oxygen, or impurities in the target, the α - α coincident events are kinematically well separated and no particle identification was needed. The outgoing α particles were therefore detected using three $50 \times 10 \text{ mm}^2$ silicon position sensitive detectors (PSD) centered at opposite sides of the beam axis at angles of 60° (PSD1), -73° (PSD2) and -103° (PSD3). The choice of these angles was determined according to the three-body kinematics for the emission of the two α particles in the quasifree assumption of a breakup process either in the target or in the projectile. In order to increase the solid angles with respect to the previous measurement [8], the detectors were placed closer to the target and covered solid angles $\Delta\Omega_1=5.5 \text{ msr}$ (PSD1) and $\Delta\Omega_2=\Delta\Omega_3=13 \text{ msr}$ (PSD2) and PSD3. The angular ranges of about 14° correspond to momentum values of the undetected ‘‘spectator’’ α particle ranging from ~ -100 MeV/ c to

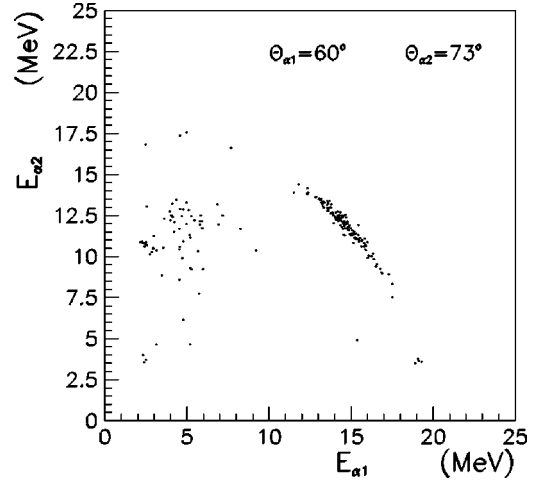


FIG. 1. The kinematic locus for the $^6\text{Li}(^6\text{Li},\alpha\alpha)^4\text{He}$ reaction at the quasifree angles of $\theta_1=60^\circ$ and $\theta_2=-73^\circ$ at beam energy of 5.67 MeV.

~ 100 MeV/ c for both QF processes. This ensures that the bulks of the two quasifree contributions fall inside the investigated regions.

Detector signals were processed by standard electronic chains and sent to the acquisition system that allowed the on-line monitoring of the experiment and the data storage on magnetic tape for off-line analysis.

IV. DATA ANALYSIS AND RESULTS

The angular calibration of the PSDs was performed by using collimators with 18 equally spaced vertical slits. Energy calibration was done by means of a standard ^{241}Am α source and of the elastic scattering on ^6Li , Au, and Cd_2 targets at higher energies. The angular resolution was found to be about 0.2° and the overall energy resolution was better than 1%.

In order to reduce the contribution of random coincidences, the time signals between any two detectors in coincidence were also recorded and the true coincidence peak was selected off line. Additionally, the requirement on the Q -value spectrum was also imposed. Figure 1 shows a typical kinematic locus for the $^6\text{Li}(^6\text{Li},\alpha\alpha)^4\text{He}$ three-body reaction, obtained at $\theta_1=60^\circ$ and $\theta_2=-73^\circ$.

In order to check the presence of the QF contribution, one-dimensional spectra have been created by plotting data versus $E_{\alpha_1}(E_{\alpha_2})$ for a given angle $\theta_1(\theta_2)$ and for different angles of the second detector, in steps of $\Delta\theta=1^\circ$, over the full angular range. An example of the resulting projections is shown in Fig. 2. A broad peak shows up that corresponds to zero-spectator momentum. The height of this peak decreases as p_α moves away from zero, as expected for a quasifree contribution (Sec. II). Similar results have been obtained for other pairs of quasifree angles. In order to further verify the nature of the peaks in Fig. 2, projections have been performed on the variables $E_{\alpha_i\alpha_j}$ (relative energy between any two α particles) to investigate the presence of possible contributions from the formation and decay of ^8Be . Such analy-

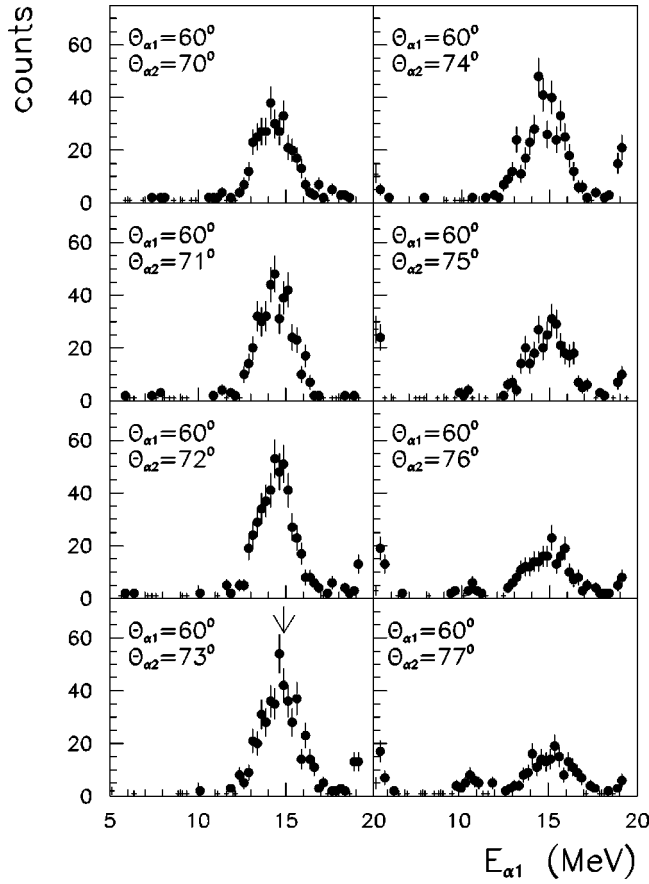


FIG. 2. Coincidence spectra projected on the E_α axis for $\theta_1 = 60^\circ$ and different θ_2 (-70° to -77°). The arrow marks the energy corresponding to the zero momentum of the spectator at the quasifree angle pair $\theta_1 = 60^\circ$ and $\theta_2 = -73^\circ$.

sis confirms that in these selected energy and angular ranges the reaction ${}^6\text{Li}({}^6\text{Li}, \alpha\alpha){}^4\text{He}$ proceeds through the QF mechanism [16–21]. There is no problem if an intermediately formed ${}^8\text{Be}$ in the final $C+c$ channel decays into the two detected α particles, because this kind of resonance would also appear in the S -factor of the astrophysical two-body reaction. The decay of a ${}^8\text{Be}$ state consisting of the spectator particle and one of the detected α particles will hardly give a significant contribution to the measured cross section for the kinematical conditions in the present experiment.

At low energies the ${}^2\text{H}({}^6\text{Li}, \alpha){}^4\text{He}$ reaction cross section is dominated by the s -wave contribution. In this case the relation to the astrophysical $S(E)$ factor is given by

$$\begin{aligned} & 4\pi \frac{s\sigma_0}{d\Omega_{\alpha_1\alpha_2}} ({}^6\text{Li}+d \rightarrow \alpha_1 + \alpha_2) \\ & = \sigma_0(E_{\text{Li}-d}) = \frac{S(E_{\text{Li}-d})}{E_{\text{Li}-d}} \exp(-2\pi n_{\text{Li}-d}). \end{aligned} \quad (19)$$

In order to extract the cross section for the ${}^4\text{He}(\alpha, {}^6\text{Li}){}^2\text{H}$ reaction appearing in Eq. (14) that is the inverse of the reac-

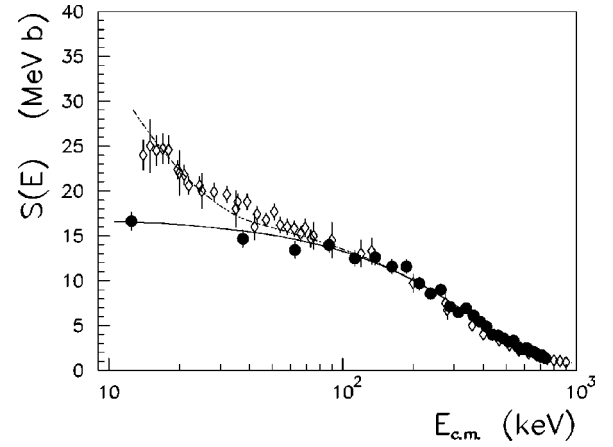


FIG. 3. The $S(E)$ factor extracted with the Trojan horse method (full dots) is compared with direct data from Ref. [12] (open dots); a fit to the indirect data with a second-order polynomial is also shown as a solid line. The fit to determine U_e is also shown (dotted line).

tion of astrophysical interest we apply the detailed balance theorem. Thus, finally, the three-body breakup cross section can be expressed as a function of the astrophysical $S(E)$ factor,

$$\begin{aligned} & \frac{d^3\sigma}{dE_{\alpha_1} d\Omega_{\alpha_1} d\Omega_{\alpha_2}} \\ & = K_F |W(\vec{Q}_{(\alpha_1\alpha_2)d})|^2 \frac{C_0}{4\pi} \frac{\mu_{\text{Li}-d} k_{\text{Li}-d}}{\mu_{\alpha_1\alpha_2} k_{\alpha_1\alpha_2}} \frac{\exp(-2\pi\eta_{\text{Li}-d})}{E_{\text{Li}-d} P_0(k_{\text{Li}-d} R)} \\ & \quad \times S(E_{\text{Li}-d}). \end{aligned} \quad (20)$$

A Monte Carlo simulation of the experiment was performed assuming a constant $S(E)$ -factor and taking into account all cuts in energy and scattering angle for the detected α particles as given by the detector setup. Additionally, only events with spectator momenta $p_\alpha < 35$ MeV/ c were selected. We assume a cutoff radius $R = 4.3$ fm that corresponds to constant $r_0 = 1.4$ fm in the parametrization

$$R = r_0 (A_{\text{Li}}^{1/3} + A_d^{1/3}). \quad (21)$$

Dividing the experimental spectrum as a function of the relative energy E_{Ax} by the simulated event spectrum directly gives the energy dependence of the astrophysical $S(E)$ factor. Statistical errors from the Monte Carlo simulation were fully included in the errors of obtained $S(E)$ factors. The indirect data were normalized to the direct data in the energy range 600–700 keV where the electron screening effects are negligible. In Fig. 3 the $S(E)$ -factor of the ${}^2\text{H}({}^6\text{Li}, \alpha){}^4\text{He}$ reaction obtained in the THM is compared with data from direct measurements [12]. Uncertainty in relative energy is estimated to be around 25 keV. Both data sets show a similar energy dependence above ≈ 100 keV while at lower energies the direct data exhibit a strong increase. This can be related to the electron screening effect (Sec. V) that is absent in the indirect measurement. In our extraction we have assumed the

TABLE I. Coefficients of a second- and third-order polynomial fit on the $S(E)$ factors, according to the different values of cutoff radius used for the calculation.

Coefficients	$R=3.69$ (fm)	$R=4.00$ (fm)	$R=4.31$ (fm)
$S(0)$ (MeV b)	15.2 ± 0.5	16.1 ± 0.5	16.9 ± 0.5
S_1 (b)	-33.25	-36.975	-39.950
S_2 (MeV ⁻¹ b)	19.984	23.588	26.067
$S(0)$ (MeV b)	14.8 ± 0.5	15.6 ± 0.5	16.6 ± 0.5
S_1 (b)	-27.9	-30.9	-35.8
S_2 (MeV ⁻¹ b)	3.7	4.9	13.3
S_3 (MeV ⁻¹ b)	14.0	16.1	11.0

dominance of the $l=0$ partial wave. At large relative energies higher partial waves will contribute to the reaction cross section. However, our $S(E)$ factor agrees well with the directly measured values for energies above approximately 100 keV, even though it was normalized to the direct data only between 600 and 700 keV. This makes our assumption quite reasonable. Significant contributions of higher partial waves at energies lower than 100 keV are rather unlikely. The $S(E)$ factor derived through the THM was fitted by a second-order polynomial of the form

$$S(E) = S(0) + S_1 E + S_2 E^2. \quad (22)$$

The best fit is shown in Fig. 3 (solid line) and its coefficients are reported in Table I together with those of a third-order polynomial. We can see no significant differences in the coefficients if we change the order of the polynomial fit. Since the Coulomb penetrability (15) depends on the choice of the cutoff radius we adopted several values of R by varying the constant r_0 in the parametrization (21). Additionally to $r_0 = 1.4$ fm we also used $r_0 = 1.3$ fm and $r_0 = 1.2$ fm that correspond to $R = 4.0$ fm and $R = 3.7$ fm, respectively. In Table I we find an astrophysical S factor at zero energy in the range $S(0) = 14.8$ – 16.9 MeV b that shows the sensitivity of the indirect method to changes in the parameter R . Since the cutoff radius R corresponds to the interaction radius in the ${}^6\text{Li}+d$ system we choose the larger value of $R = 4.3$ fm, in agreement with Ref. [24]. The corresponding value of $S(0) = (16.9 \pm 0.5)$ MeV b is slightly smaller than the value $S(0) = 17.4$ MeV b extrapolated from direct measurements of the cross section [12] after correcting for the electron screening effect. Besides the cutoff radius R , the extracted S factor depends on the assumed shape of the momentum distribution $|\Phi_{\text{Li}}|^2$. Since we use a small momentum cutoff only the peak region of the distribution is employed, which is quite independent of the exact form of the ${}^6\text{Li}$ ground state wave function.

V. ELECTRON SCREENING EFFECT

For nuclear reactions studied in the laboratory, the target and the projectile nuclei are always bound in neutral atoms or molecules and ions. Interaction of the nuclides with their electron clouds will cause the electron screening effect en-

TABLE II. Comparison between screening potential U_e extracted via THM for ${}^6\text{Li}+d$ (present work) and ${}^7\text{Li}+p$ [25].

	${}^6\text{Li}+d \rightarrow \alpha + \alpha$	${}^7\text{Li}+p \rightarrow \alpha + \alpha$	Adiabatic limit
U_e (eV)	340 ± 51	~ 350	186

hancing the “bare” $S(E)$ factor at low energies by a factor $e(\pi\eta U_e/E)$ (see Ref. [12]). The expected enhancement has been observed in several fusion reactions (see Ref. [25] and references therein) and was much larger than the adiabatic limit, i.e., the difference in electron binding energies between the colliding atoms and the compound system. Possible solution for this discrepancy might be found in one or more of the following areas: (1) the assumed energy-loss predictions at low energies, (2) the assumed nuclear reaction models at energies far below the Coulomb barrier, and (3) the assumed atomic-physics models.

The THM can provide an independent and experimental test of area (2) because it allows us to measure the bare astrophysical factor S_b , which can be compared with the screened (direct) value S_d [12] in order to extract the associated screening potential energy U_e using

$$S_d = S_b \exp\left(\frac{\pi\eta U_e}{E}\right). \quad (23)$$

In fact, the energy dependence of $S_b(E)$ should be identical to that derived by direct measurements, except at low energies ($E/U_e < 100$), where the two data sets should differ due to the effects of electron screening. Moreover, from the comparison of direct and THM data we are able to have a measure of U_e independent of the model for electron screening. Of course, the extracted screening potential energy U_e depends on the approximations used in the THM.

That is done for the present data set (Fig. 3), leading to $U_e = 340 \pm 51$ eV. This value is in agreement with the results of Ref. [12] and is much larger than 186 eV, predicted by the adiabatic approximation for the $\text{Li}+d$ case (see Table II). This kind of analysis was already performed for ${}^7\text{Li}+p \rightarrow \alpha + \alpha$, where we found $U_e \sim 350$ eV [25]. It is important to stress the complementarity between the THM and direct measurements to have hints on the low energy trend of astrophysically relevant cross sections and the electron screening effect.

VI. CONCLUSIONS

The present work investigates a possible way of measuring the astrophysical $S(E)$ factor at energies relevant for astrophysical applications by means of the Trojan horse method. The energy dependence of the astrophysical $S(E)$ factor can be directly deduced by measuring the cross section of a suitably chosen reaction with three particles in the final state. The strong energy dependence in the cross section of the astrophysically relevant two-body reaction due to the Coulomb barrier is removed by penetrability factors in the cross section of the three-body reaction. We have used a simple approximation for the integral that appears in the postform PWBA within the surface approximation. The

THM can help to overcome the problems connected with the extraction of the bare nucleus cross section from the shielded nucleus cross section, which is measured in direct experiments. Alternatively the THM can be regarded as an independent tool to investigate the effects of electron screening by comparing the cross section for bare nuclei from the THM with the cross section from direct measurements.

ACKNOWLEDGMENTS

It is a pleasure to acknowledge the precious collaboration given by Dr. M. Jaksić during the experiment and the kind hospitality received at the Rudjer Bošković Institute. The smooth operation of the Tandem accelerator and connected facilities is also gratefully acknowledged.

-
- [1] G. Baur and H. Rebel, *J. Phys. G* **20**, 1 (1994), and references therein.
 - [2] G. Baur and H. Rebel, *Annu. Rev. Nucl. Part. Sci.* **46**, 321 (1996).
 - [3] J. G. Ross, G. Görres, C. Iliadis, S. Vouzoukas, M. Wiescher, R. B. Vogelaar, S. Utku, N. P. T. Bateman, and P. D. Parker, *Phys. Rev. C* **52**, 1681 (1995).
 - [4] C. A. Gagliardi, R. E. Tribble, A. Azhari, H. L. Clark, Y. W. Lui, A. M. Mukhamedzhanov, A. Sattarov, L. Trache, V. Burjan, J. Cejpek, V. Kroha, S. Piskor, and J. Vincour, *Phys. Rev. C* **59**, 1149 (1999).
 - [5] A. Azhari, V. Burjan, F. Carstoiu, H. Dejbakhsh, C. A. Gagliardi, V. Kroha, A. M. Mukhamedzhanov, L. Trache, and R. E. Tribble, *Phys. Rev. Lett.* **82**, 3960 (1999).
 - [6] A. N. Ostrowsky, A. C. Shotter, W. Bradfield-Smith, A. M. Laird, A. Di Pietro, T. Davinson, S. Monroe, P. J. Woods, S. Cherubini, W. Galster, J. S. Graulich, P. Leleux, L. Michel, A. Ninane, J. Vervier, M. Aliotta, C. Cali, F. Cappuzzello, A. Cunsolo, C. Spitaleri, J. Görres, M. Wiescher, J. Rahighi, and J. Hinnefeld, *Nucl. Part. Phys.* **24**, 1553 (1998).
 - [7] G. Baur, *Phys. Lett.* **78B**, 35 (1986).
 - [8] S. Cherubini, V. N. Kondratyev, M. Lattuada, C. Spitaleri, D. Miljanić, M. Zadro, and G. Baur, *Astrophys. J.* **457**, 855 (1996).
 - [9] C. Spitaleri, M. Aliotta, S. Cherubini, M. Lattuada, D. Miljanić, S. Romano, N. Soić, M. Zadro, and R. A. Zappalà, *Phys. Rev. C* **60**, 055802 (1999).
 - [10] G. Calvi, S. Cherubini, M. Lattuada, S. Romano, C. Spitaleri, M. Aliotta, G. Rizzari, M. Sciuto, R. A. Zappalà, V. N. Kondratyev, D. Miljanić, M. Zadro, G. Baur, O. Yu. Goryunov, and A. A. Shvedov, *Nucl. Phys.* **A621**, 139c (1997).
 - [11] C. Rolfs and R. W. Kavanagh, *Nucl. Phys.* **A455**, 179 (1986).
 - [12] S. Engstler, G. Raimann, C. Angulo, U. Greife, C. Rolfs, U. Schröder, E. Somorjai, B. Kirch, and K. Langanke, *Z. Phys. A* **342**, 471 (1992).
 - [13] C. Spitaleri, M. Aliotta, P. Figuera, M. Lattuada, R. G. Pizzone, S. Romano, A. Tumino, C. Rolfs, L. Gialanella, F. Strieder, S. Cherubini, A. Musumarra, D. Miljanić, S. Typel and H. H. Wolter, *Eur. Phys. J. A* **7**, 181 (2000).
 - [14] S. Typel and H. H. Wolter, *Few-Body Syst.* **29**, 75 (2000).
 - [15] G. R. Satchler, *Introduction to Nuclear Reactions*, 2nd ed. (MacMillan, London, 1990).
 - [16] N. S. Chant and P. G. Roos, *Phys. Rev. C* **15**, 57 (1977).
 - [17] L. L. Gadeken and E. Norbeck, *Phys. Rev. C* **6**, 1172 (1972).
 - [18] S. Barbarino, M. Lattuada, F. Riggi, C. Spitaleri, and D. Vinciguerra, *Phys. Rev. C* **21**, 1104 (1980).
 - [19] E. Norbeck, C. R. Caen, N. D. Strathman, and D. A. Fox, *Phys. Rev. C* **23**, 2557 (1981).
 - [20] M. Lattuada, F. Riggi, C. Spitaleri, D. Vinciguerra, X. Aslanoglou, G. Vourovopoulos, and D. Miljanić, *Phys. Rev. C* **30**, 531 (1984).
 - [21] M. Lattuada, F. Riggi, C. Spitaleri, D. Vinciguerra, and D. Miljanić, *Z. Phys. A* **328**, 497 (1987).
 - [22] M. Lattuada, F. Riggi, C. Spitaleri, D. Vinciguerra, G. Vourovopoulos, D. Miljanić, and E. Norbeck, *Z. Phys. A* **330**, 1848 (1988), and references therein.
 - [23] I. Slaus, R. G. Allas, L. A. Beach, R. O. Bondelid, E. L. Petersen, J. M. Lambert, P. A. Treado, and R. A. Moyle, *Nucl. Phys.* **A286**, 67 (1977).
 - [24] R. D. Evans, *The Atomic Nucleus* (McGraw-Hill, New York, 1969).
 - [25] M. Aliotta, C. Spitaleri, M. Lattuada, A. Musumarra, R. G. Pizzone, A. Tumino, C. Rolfs, and F. Strieder, *Eur. Phys. J. A* **9**, 435 (2000).